Broad Detecting Range of Objective-Based Surface Plasmon Resonance Sensor via Multilayer Structure

2011 Jpn. J. Appl. Phys. 50 09MG04

(http://iopscience.iop.org/1347-4065/50/9S1/09MG04)

Japanese Journal of Applied Physics **50** (2011) 09MG04 **BRIEF NOTE**
DOI: 10.1143/JJAP.50.09MG04

Broad Detecting Range of Objective-Based Surface Plasmon Resonance Sensor via Multilayer Structure

Tzu-Hsiang Lan, Yi-Kuan Chung, and Chung-Hao Tien[1]*

Department of Photonics and Institute of Electro-optical Engineering, National Chiao Tung University, Hsinchu 30010, Taiwan
[1] *Department of Photonics and Display Institute, National Chiao Tung University, Hsinchu 30010, Taiwan*

Received February 13, 2011; accepted May 30, 2011; published online September 20, 2011

The demand of pursuing higher resolution drives the instrumental development of a surface plasmon resonance (SPR) sensor to shift from Kretchmann to objective-based configuration. However, its maximum sensing refractive index is restricted by the numerical aperture of an objective lens. Based on the mode conversion, we proposed a multilayer structure to extend the detecting range up to 11% (from 1.28 to 1.42) for a 1.45 objective lens via a transformed SPR mode. This technique not only overcomes intrinsic constraint but also reduces the cost.

Surface plasmon resonance (SPR) sensors have been widely used to analyze characteristics of materials, providing quantitative and qualitative analyses.[1)] The trends of development of SPR sensors have changed from conventional prism-based toward an objective-based platform owing to the advantages of scan-free operation, smaller detecting area, and higher surface plasmon polaritons (SPPs) conversion efficiency when used in conjunction with a radial polarization.[2–4)] As a result, several studies have been performed on objective-based SPR sensors with radial polarization to form a cell image containing fine details and high contrast based on a two-dimensional refractive index map.[5,6)]

However, the combination of objective-based SPR sensors with radial polarization still has not been widely used owing to essential constraints. The main issue is that the maximum detecting value of refractive index is restricted by the numerical aperture (NA) of the immersion objective lens.[6)] For example, a 1.45 NA immersion lens, having a maximum half convergence angle of 75.16°, can only detect samples with a refractive index smaller than 1.28. Therefore, it is vital to overcome this essential constraint for the objective-based SPR sensor. In this study, we utilized a transformed SPR mode to extend the detecting range of refractive index via a multilayer structure. Under a fixed 1.45 NA objective lens, the detecting range can be increased by 11% up to 1.42, which covers the general usage for biomolecular detection.

The optical configuration and proposed metal–insulator–metal (MIM) structure are shown in Fig. 1(a). The radially polarized light ($\lambda = 632.8\,\text{nm}$) is focused on a MIM structure by an immersion objective lens with NA = 1.45. The symmetric MIM structure [gold ($d_1, \varepsilon = -9.8 + 1.96i$)–SiO$_2$ ($d_2, n = 1.46$)–gold (d_1)] was sandwiched by the cover slip ($n = 1.5$) and the test sample (n_4). Then, the reflected light is collected by the same objective lens and projected to its back pupil onto a charge-coupled device (CCD), as shown in Fig. 1(b) for the case of a MIM with $d_2 = 0$ and $n_4 = 1$.

As the beam is focused on the multilayer structure, not only the cavity resonance (CR) mode but also the SPR mode is generated.[7)] By performing the equation of multiple reflection, a plot of angular reflectance accurately predicted the resonance angles of the two modes. Figure 2 shows the change in angular reflectance with respect to different thicknesses of SiO$_2$ in a water-attached MIM structure. CR and SPR modes are classified according to the critical angle of the sample–gold interface (vertical dashed line). For sensing purposes, the CR mode has no contribution, but it becomes useful when it converts into a transformed SPR (T-SPR) mode. The resonance dip of the CR mode gradually moves toward a higher angular position when the thickness of the insulator is increased. When the dip of the CR mode exceeds the critical angle (the critical thickness of SiO$_2$ is 255 nm), the CR mode is able to convert to the T-SPR mode. In the meantime, the dispersion curve of a CR mode intersects with that of an SPR mode owing to the increase in the wave vector of the CR mode caused by the superposition of multiple reflections.

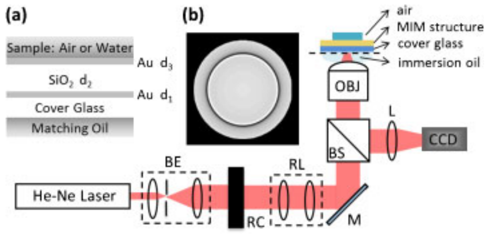

Fig. 1. (Color online) Optical configuration of objective-based SPR sensor, where BE: beam expander, RC: radial converter, RL: relay lens, M: mirror, BS: beam splitter, OBJ: objective lens, and CCD: charge-coupled device. (a) MIM structure. (b) Field distribution of the reflected beam at the exit pupil.

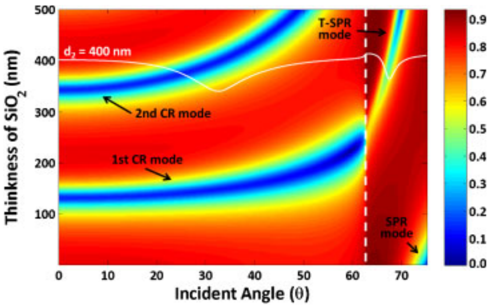

Fig. 2. (Color online) Change in angular reflectance with respect to different SiO$_2$ thicknesses in a water-attached MIM structure. The vertical dashed line is the critical angle and the reflectance curve of $d_2 = 400\,\text{nm}$ is highlighted with a solid line.

To illustrate the sensitivity of the T-SPR mode, we have varied the thickness of the test sample on the basis of multiple reflection calculation. Figure 3(a) shows the change in angular reflectance with respect to the different thick-

---

*E-mail address: chtien@mail.nctu.edu.tw

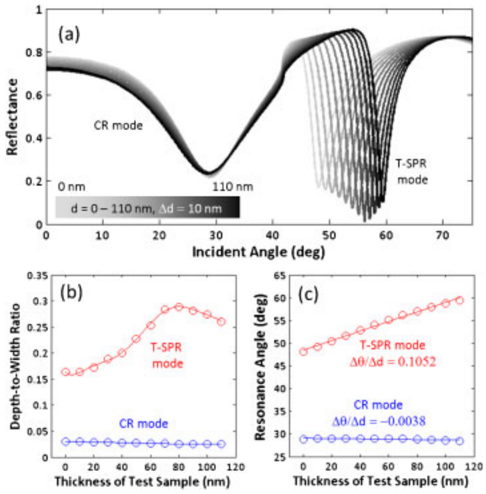

Fig. 3. (Color online) (a) Change in angular reflectance with respect to the thickness of the test sample ($n = 1.33$) from 10 to 110 nm. (b) DWR and (c) sensitivity of the CR mode and the T-SPR mode.

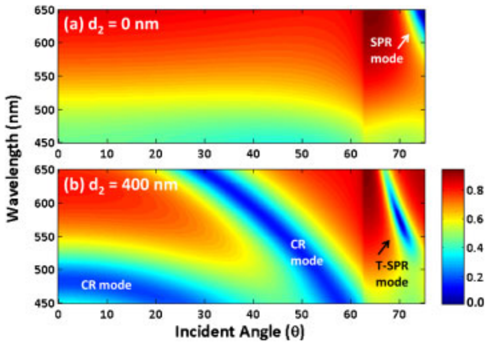

Fig. 4. (Color online) Comparison of angular reflectance over a wide wavelength range between (a) MIM with $d_2 = 0$ nm and (b) MIM with $d_2 = 400$ nm.

nesses of the sample layer ($n = 1.33$). The contrast and sensitivity of different modes are respectively shown in Figs. 3(b) and 3(c). By using the depth-to-width ratio (DWR) to define the contrast of the reflected signal, it is clearly shown that the averaged DWR magnitude of the T-SPR mode is 8.5 times larger than that of the CR mode. Furthermore, the T-SPR mode provides an obvious angular shift with linear dependence on sensitivity, which is 27.6 times larger than that of the CR mode. As a result, the T-SPR mode is superior to the CR mode for sensing applications.

The thickness of gold thin films determines the guiding efficiency of CR modes and the transfer efficiency from a CR mode to a T-SPR mode. The thickness of the top gold monolayer (d_3) affects the angular position of T-SPR modes as well as its signal contrast. For optimization, we set a coupler with the parameters of gold ($d_1 = 20$ nm)–SiO$_2$ ($d_2 = 400$ nm)–gold ($d_3 = 20$ nm) for working wavelength $\lambda = 632.8$ nm. The proposed multilayer structure can not only extend the detecting range of refractive index but also universally operate over a certain wavelength range. As shown in Fig. 4(b), the MIM structure provides a sharp T-SPR mode in a wide range of working wavelength. Compared with original SPR modes [Fig. 4(a)], the DWR of the T-SPR mode dips increased 357% (0.060 → 0.214) at $\lambda = 530$ nm and 278% (0.018 → 0.050) at $\lambda = 450$ nm. This provides a promising potential for the wavelength sweeping operation.

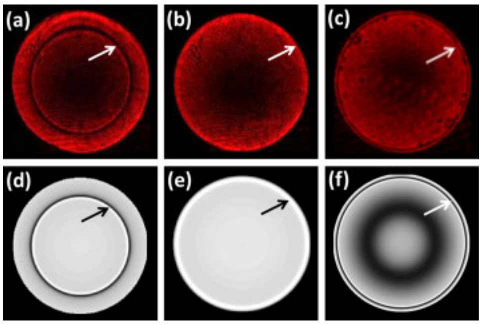

Fig. 5. (Color online) Comparison between (a)–(c) experimental results and (d)–(f) simulation results for MIM structure attached to different test samples: (a) air-attached MIM with $d_2 = 0$ nm, (b) water-attached MIM with $d_2 = 0$ nm, and (c) water-attached MIM with $d_2 = 400$ nm.

Finally, a comparison between experimental results and simulation results for different conditions is given. Figure 5(a) shows a typical reflected disk captured on the back pupil plane in the case of a gold monolayer attached to air. When the test sample was changed to water, the dark resonance ring lies outside the exit pupil and only remains a bright ring on the border, which is refer to total internal reflection, as shown in Fig. 5(b). Figure 5(c) clearly shows that the sensing range of refractive index can be equivalently extended from 1.28 to 1.42 via the MIM structure. The experimental results confirmed the simulation predication that T-SPR modes do enlarge the detection window in a 1.45 NA objective lens.

In conclusion, a MIM structure was proposed to overcome the barrier of detecting limitation of an objective-based SPR sensor due to the limited NA of an objective lens. Based on mode conversion, the T-SPR modes provides an additional 11% observation window (up to 1.42) for a 1.45 NA objective lens covering the general usage for biomolecules. Also, T-SPR modes have sharper resonant dips over a wide range of working wavelength promising a sweeping operation in frequency. We believe that the proposed idea can push technology forward and enhance the capability of the objective-based SPR sensor to investigate the physical properties of biomacromolecules and protein–protein interactions.

Acknowledgements The financial support from the National Science Council, Taiwan, under contract NSC 99-2221-E-009-067-MY3 and AU Optronics Corporation is acknowledged.

1) J. Homola: Chem. Rev. **108** (2008) 462.
2) E. Kretschmann and H. Raether: Z. Naturforsch. A **23** (1968) 2135.
3) G. Stabler, M. G. Somekh, and C. W. See: J. Microsc. **214** (2004) 328.
4) Q. Zhan: Opt. Lett. **31** (2006) 1726.
5) K. J. Moh, X. C. Yuan, J. Bu, S. W. Zhu, and B. Z. Gao: Opt. Express **16** (2008) 20734.
6) K. J. Moh, X. C. Yuan, J. Bu, S. W. Zhu, and B. Z. Gao: Opt. Lett. **34** (2009) 971.
7) R. Zhao, T. Zhai, Z. Wang, Y. Wang, and D. Liu: Appl. Phys. B **92** (2008) 585.